OPEN ACCESS
Journal of Theoretical and Computational Acoustics
Vol. 29, No. 3 (2021) 2150004 (22 pages)

DOI: 10.1142/S2591728521500043

Low-Rank Iteration Schemes for the Multi-Frequency Solution of Acoustic Boundary Element Equations

Suhaib Koji Baydoun*,‡, Matthias Voigt† and Steffen Marburg*

Chair of Vibroacoustics of Vehicles and Machines
Department of Mechanical Engineering, Technische Universität München
Boltzmannstraße 15, 85748 Garching, Germany

†*Fachbereich Mathematik, Bereich Optimierung und Approximation*
Universität Hamburg, Bundesstraße 55, 20146 Hamburg, Germany

Institut für Mathematik, Technische Universität Berlin
Straße des 17. Juni 136, 10623 Berlin, Germany
‡*Suhaib.Baydoun@tum.de*

Received 10 December 2020
Revised 11 February 2021
Accepted 11 March 2021
Published 8 May 2021

The implicit frequency dependence of linear systems arising from the acoustic boundary element method necessitates an efficient treatment for problems in a frequency range. Instead of solving the linear systems independently at each frequency point, this paper is concerned with solving them simultaneously at multiple frequency points within a single iteration scheme. The proposed concept is based on truncation of the frequency range solution and is incorporated into two well-known iterative solvers - BiCGstab and GMRes. The proposed method is applied to two acoustic interior problems as well as to an exterior problem in order to assess the underlying approximations and to study the convergence behavior. While this paper provides the proof of concept, its application to large-scale acoustic problems necessitates efficient preconditioning for multi-frequency systems, which are yet to be developed.

Keywords: Boundary element method; multi-frequency; low-rank; iterative solver.

1. Introduction

The boundary element method (BEM) is a popular numerical method for the discretization of the acoustic Helmholtz equation.[1–3] Compared to the finite element method (FEM),[4]

‡Corresponding author.

BEM reduces the spatial dimension of the problem by one and hence, boundary element (BE) discretizations only involve the surface of the acoustic domain. However, although resulting in a significantly smaller number of equations, BEM is not necessarily more efficient than FEM in terms of computational time, particularly for large-scale problems.[5] Among others, this is attributed to the implicit frequency dependence of BE coefficient matrices. In contrast, acoustic FEM usually yields a linear system of equations with quadratic frequency dependence, which admits efficient approximation by Krylov subspace methods[6] or even the computation of modal quantities by standard eigensolvers.[7] Clearly, the situation is different in the case of BEM, and more elaborate approaches are required in order to alleviate the high computational effort that is required for problems with rapidly varying responses.

The first approaches for efficient BE analyses over frequency ranges were based on computing the BE matrices only at a few sample frequencies and linear interpolations in between,[8] or based on truncated Taylor series.[9] Wu *et al.* suggested a frequency interpolation of the Green's function, thereby limiting the numerical integration to a single frequency.[10] Such frequency approximations of BE matrices also paved the way to acoustic eigenvalue analyses with BEM.[11–13] More recently, Chebyshev approximations[14] and rational Cauchy approximations[15] of the system matrix have been proposed in the context of modal analyses with BEM.

Instead of using frequency approximations of the system matrix, the acoustic response itself may be approximated as well. Examples include the evaluation of the sound pressure at a single field point as well as the computation of integrated quantities such as radiated sound power. Coyette *et al.,* employed a Padé approximation to extend the response from a single BE solution to a range of frequencies.[16] Similar methods have also been applied to transfer matrices for an efficient multi-frequency calculation of radiated sound power.[17,18]

While frequency approximations of BE matrices only address the effort for setting-up the coefficient matrices, the solution of the linear system accounts for a major share in the overall computational effort as well. Acoustic problems with only a few degrees of freedom (DOF) can be efficiently solved by Gaussian elimination. However, most of today's engineering problems are addressed by means of iterative solvers such as Krylov subspace methods[19] requiring repeated evaluations of matrix vector products. While solving a sequence of linear systems, the total number of matrix vector products can be significantly reduced by reusing selected subspaces.[20,21] Moreover, the high complexity associated with the evaluation of products involving fully populated matrices have been addressed by several fast algorithms[22,23] that have also been combined with efficient multi-frequency strategies.[24] In recent years, frequency-sweep analyses of vibroacoustic problems have also been accelerated by means of model order reduction.[15,25–27]

This paper is concerned with solving linear systems arising from acoustic BEM simultaneously at multiple frequency points within a single iteration scheme. The evaluation of the matrix vector products is accelerated by compressing the frequency range information by low-rank truncations. Essentially, the low-rank truncations exploit the fact that the spatial patterns of acoustic responses usually feature regularity with respect to the frequency — a concept that also underlies model order reduction techniques such as modal

superposition. Several iterative schemes relying on the low-rank format have been proposed in the context of solving parametrized linear systems, and a summary can be found in the survey by Grasedyck *et al.*[28] In the authors' preliminary work,[29] a low-rank version of BiCGstab has been applied to an acoustic interior problem. This paper extends that work to the low-rank GMRes method and provides insights with regard to approximation errors, convergence behavior and computational times. The approach in this paper is based on the works by Kressner and Tobler[30] as well as the work of Ballani and Grasedyck[31] on the iterative solution of high-dimensional linear systems. Though only the frequency dependence is considered in this paper, the general concept can be straightforwardly applied to other parameter dependencies such as those originating from vibroacoustic optimization problems[32] and uncertainty quantification.[33] The main objective of this paper is to demonstrate the application of low-rank approximations in the context of acoustic BEM and to provide a proof of concept.

Section 2 outlines the proposed method. Low-rank factorizations in conjunction with a frequency approximation of the BE system matrix enable efficient evaluations of matrix vector products within iterative schemes. These concepts are described in detail and incorporated into the biconjugate gradient stabilized method (BiCGstab) and the generalized minimal residual method (GMRes). Section 3 then provides the proof of concept based on two acoustic interior problems as well as an exterior problem. The underlying approximations, i.e. the low-rank factorizations and the frequency interpolation, are assessed systematically, the convergence behaviors of low-rank versions of BiCGstab and GMRes are studied, and the computational times are compared to those of a conventional frequency-wise strategy. In Sec. 4, the paper concludes with an outlook on possible improvements of the method in order to extend its applicability to a wide range of engineering problems in the future.

2. Low-Rank Solvers for the Acoustic Boundary Element Method

Boundary element formulations are often categorized into directed and indirect approaches.[1–3] This work exclusively considers the direct formulation, in which the Kirchhoff–Helmholtz integral equation is obtained by application of Green's theorem. The integral equation and associated boundary conditions can be discretized by several methods, of which collocation and Galerkin discretization methods are the most popular ones. Though only direct collocation BEM is considered in what follows, the iteration scheme proposed in this section is straightforwardly applicable to other frequency-dependent linear systems as well. The resulting linear system of equations reads

$$\mathbf{H}(k)\mathbf{p} = \mathbf{G}(k)\mathbf{v} + \mathbf{p}_\mathrm{i} = \mathbf{b}(k), \quad \mathbf{H}(k), \mathbf{G}(k) \in \mathbb{C}^{n\times n}, \quad \mathbf{p}, \mathbf{v}, \mathbf{p}_\mathrm{i}, \mathbf{b}(k) \in \mathbb{C}^{n\times 1}. \tag{1}$$

The complex-valued matrices $\mathbf{H}(k)$ and $\mathbf{G}(k)$ are obtained by element-wise numerical integration. They are implicitly dependent on the wavenumber $k = 2\pi f/c$, where f is the frequency and c denotes the speed of sound. They are both fully populated, and generally neither positive definite nor Hermitian. The matrix $\mathbf{H}(k)$ contains the integral-free term of the Kirchhoff–Helmholtz integral equation as well as the contributions of the double layer

potential and the admittance boundary condition. Further, $\mathbf{G}(k)$ corresponds to the single layer potential. The vector $\mathbf{p}$ contains unknown nodal scalar sound pressure values, and the excitation is given by the vector of nodal scalar particle velocities $\mathbf{v}$ as well as the incident pressure field $\mathbf{p}_\mathrm{i}$. Usually, the right-hand side vector $\mathbf{b}(k)$ is assembled directly in order to avoid the storage of the fully populated matrix $\mathbf{G}(k)$. Each node carries a single DOF, and hence n refers to the number of nodes as well as to the number of unknowns.

Many vibroacoustic applications are subject to excitation at a range of frequencies, and hence the simulation of their acoustic responses with BEM requires setting up and solving linear systems at each frequency point of interest, i.e. wavenumbers $k_1, \ldots, k_m$. Usually, the m linear systems are successively solved by either direct or iterative solvers. Linear systems with only a few DOFs can be solved directly by computing a system matrix factorization. For a single frequency solution, this is associated with an algorithmic complexity of $\mathcal{O}(n^3)$. However, most of today's engineering problems are addressed by means of iterative solvers, which rely on repeated evaluation of matrix vector products. Hence, the use of iterative solvers reduces the algorithmic complexity to $\mathcal{O}(n^2)$ for a single frequency solution, given that convergence is reached in a few iterations. The total number of matrix vector multiplications determines the computational effort of the individual solution process. Clearly, the overall computational effort is significantly driven by the number of frequency points. The main idea behind the proposed iterative scheme is to enhance the numerical efficiency of those matrix vector multiplications by making use of low-rank approximations.

Instead of solving the m linear systems resulting from acoustic BEM individually, they can be arranged in a single system with a block diagonal system matrix. The solution vectors and right-hand sides corresponding to the m frequency points are vertically concatenated, which gives

$$\begin{bmatrix} \mathbf{H}(k_1) & & \\ & \ddots & \\ & & \mathbf{H}(k_m) \end{bmatrix} \begin{bmatrix} \mathbf{p}_1 \\ \vdots \\ \mathbf{p}_m \end{bmatrix} = \begin{bmatrix} \mathbf{b}(k_1) \\ \vdots \\ \mathbf{b}(k_m) \end{bmatrix}. \tag{2}$$

As mentioned above, products similar to the one on the left-hand side of Eq. (2), which require multiplication of the system matrix with an intermediate (i.e. not yet converged) solution vector, occur repeatedly in iterative schemes. The objective is to define an efficient procedure for their evaluation. For this, the sound pressure vectors $\mathbf{p}_1, \ldots, \mathbf{p}_m$, corresponding to the intermediate solutions at the desired wavenumbers $k_1, \ldots, k_m$, are rearranged side by side in the matrix $\mathbf{P} = [\mathbf{p}_1, \ldots, \mathbf{p}_m]$, hence $\mathbf{P} \in \mathbb{C}^{n \times m}$. Once convergence is reached, it can be interpreted as a matrix containing the frequency range solution. For the sake of readability, $\mathbf{P}$ will be simply referred to as solution matrix in the remainder of the paper, though it serves as representative for all intermediate matrices that arise over the course of the iterations.

The key concept of the proposed method relies on finding a low-rank approximation of the matrix $\mathbf{P}$ and thereby compressing the frequency range information. Assuming a singular value decomposition (SVD) and subsequent truncation, an approximation of $\mathbf{P}$ can

be written as the product of two *tall-and-skinny* matrices, i.e.

$$\mathbf{P} \approx \mathbf{U_P}\mathbf{V_P}^{\mathrm{H}}, \quad \mathbf{U_P} \in \mathbb{C}^{n\times r}, \quad \mathbf{V_P} \in \mathbb{C}^{m\times r}, \tag{3}$$

with the rank $r \ll n, m$. The superscript $(\cdot)^{\mathrm{H}}$ denotes the Hermitian transpose of a matrix. Details on this low-rank factorization are given in Sec. 2.1.

Moreover, a frequency approximation of the BE system matrix is introduced as second approximation. It is defined such that

$$\mathbf{H}(k) \approx \sum_{j=0}^{q} \mathbf{H}_j v_j(k), \tag{4}$$

is approximated by a linear combination of a few frequency-independent coefficient matrices $\mathbf{H}_j$. They are multiplied with the scalar-valued, frequency-dependent functions $v_j(\cdot)$ as weights. For the efficiency of the method, the number of terms is required to be small, i.e. $q \ll n, m$. Details on the construction of the approximation in Eq. (4) are provided in Sec. 2.2.

Furthermore, the right-hand side vectors at the desired wavenumbers are also rearranged in the matrix $\mathbf{B} = [\mathbf{b}(k_1), \ldots, \mathbf{b}(k_m)]$, similar to the definition of the solution matrix $\mathbf{P}$. Finally, with the approximations in Eqs. (3) and (4) at hand, a linear operator $\boldsymbol{\mathcal{H}} : \mathbb{C}^{n\times m} \to \mathbb{C}^{n\times m}$ is introduced as

$$\boldsymbol{\mathcal{H}}(\mathbf{P}) = \sum_{j=0}^{q} (\mathbf{H}_j \mathbf{U_P})(\mathbf{V_P}^{\mathrm{H}} \mathbf{D}_j), \quad \mathbf{D}_j = \mathrm{diag}(v_j(k_1), \ldots, v_j(k_m)). \tag{5}$$

Application of $\boldsymbol{\mathcal{H}}$ to the solution matrix $\mathbf{P}$ approximately yields the right-hand side matrix $\mathbf{B}$ at a computational effort of $\mathcal{O}(qr(n^2 + m + mn))$. It serves as an alternative for evaluating the matrix vector product on the left-hand side of Eq. (2) which would require $\mathcal{O}(mn^2)$ number of operations. Hence, the evaluation via Eq. (5) is economic when $qr < m$, which holds as long as one is interested in a fine frequency resolution, and the approximations in Eqs. (3) and (4) yield sufficient accuracy with only small numbers of terms. The numerical examples in Sec. 3 verify the latter assumption.

2.1. *Low-rank factorization*

A factorization of the solution matrix $\mathbf{P} \in \mathbb{C}^{n\times m}$ as given in Eq. (3) with a small rank is crucial for the efficiency of the operation in Eq. (5). Its computation is described in what follows.

The rank R of a matrix corresponds to the number of linearly independent rows and columns, and a matrix is said to have full rank if $R = \min(n, m)$. Assuming an irregular spatial distribution of the sound pressure field and also an absence of any regularity of the sound pressure with respect to the frequency, $\mathbf{P}$ would originally have full rank. However, in most applications this is not the case, and $\mathbf{P}$ admits a sufficiently accurate approximation by a matrix of significantly reduced rank r compared to the original rank, i.e. $r \ll R$. Actually, this is also the underlying concept of modal superposition, in which the response

in a frequency range is expressed as a summation of a few modes of the system. However, the proposed method does not rely on the solution of an eigenvalue problem that would be required to determine the modes.

For a given rank r, the closest approximation of a matrix with respect to the Frobenius norm is achieved by SVD and subsequent truncation. Since $\mathbf{P}$ is nonsquare (i.e. $m \neq n$), the economic version of SVD is used in this paper, which omits the rows or columns of zeros from the singular value matrix. The algorithm for computing the SVD is based on bidiagonalization and is associated with a complexity of $\mathcal{O}(nm^2)$ when $m < n$. The resulting factorization reads

$$\mathbf{P} = \tilde{\mathbf{U}}_{\mathbf{P}} \Sigma_{\mathbf{P}} \tilde{\mathbf{V}}_{\mathbf{P}}^{\mathrm{H}}, \tag{6}$$

where $\Sigma_{\mathbf{P}}$ is a diagonal matrix containing the real-valued, nonnegative singular values $\sigma_1 \geq \cdots \geq \sigma_R$ in decreasing order. Given an analytical frequency dependence of the system matrix $\mathbf{H}(k)$ and right-hand side $\mathbf{b}(k)$, it is proven that the singular values of $\mathbf{P}$ exhibit exponential decay.[30] This also confirms the admissibility of approximating $\mathbf{P}$ with a low-rank factorization. Instead of defining a fixed rank for the truncation, a relative error $\epsilon_{\mathcal{T}}$ is chosen, and the smallest r is found such that

$$\sqrt{\sigma_{r+1}^2 + \cdots + \sigma_R^2} \leq \epsilon_{\mathcal{T}} \sqrt{\sigma_1^2 + \cdots + \sigma_r^2}. \tag{7}$$

Thereby, the error in the Frobenius norm, introduced due to the approximation $\mathbf{P} \approx \mathbf{U}_{\mathbf{P}} \mathbf{V}_{\mathbf{P}}^{\mathrm{H}}$, is limited to $\left\|\mathbf{P} - \mathbf{U}_{\mathbf{P}} \mathbf{V}_{\mathbf{P}}^{\mathrm{H}}\right\|_{\mathrm{F}} \leq \epsilon_{\mathcal{T}} \|\mathbf{U}_{\mathbf{P}} \mathbf{V}_{\mathbf{P}}^{\mathrm{H}}\|_{\mathrm{F}}$. With the rank r at hand, $\mathbf{U}_{\mathbf{P}}$ and $\mathbf{V}_{\mathbf{P}}$ are constructed using the corresponding singular vectors $\tilde{\mathbf{u}}$ and $\tilde{\mathbf{v}}$ of $\tilde{\mathbf{U}}_{\mathbf{P}}$ and $\tilde{\mathbf{V}}_{\mathbf{P}}$, i.e.

$$\mathbf{U}_{\mathbf{P}} = [\tilde{\mathbf{u}}_1, \ldots, \tilde{\mathbf{u}}_r]\mathrm{diag}(\sqrt{\sigma_1}, \ldots, \sqrt{\sigma_r}), \quad \mathbf{V}_{\mathbf{P}} = [\tilde{\mathbf{v}}_1, \ldots, \tilde{\mathbf{v}}_r]\mathrm{diag}(\sqrt{\sigma_1}, \ldots, \sqrt{\sigma_r}). \tag{8}$$

In this way, the truncation operator $\boldsymbol{\mathcal{T}} : \mathbb{C}^{n \times m} \to \mathbb{C}^{n \times m}, \mathbf{P} \mapsto \mathbf{U}_{\mathbf{P}} \mathbf{V}_{\mathbf{P}}^{\mathrm{H}}$ can be defined. Thereby calculated low-rank factorizations play an important role in the iterative schemes described in Sec. 2.3.

2.2. *Frequency approximation of the boundary element equations*

Beside the above-described low-rank factorization, a frequency approximation of the system matrix $\mathbf{H}(k)$ is the second essential approximation underlying the proposed iterative scheme. The form in Eq. (4) is given by a linear combination of a few frequency-independent coefficient matrices and should enable satisfactory approximation over the whole frequency range of interest. Different types of polynomial[12,14] and rational approximations[15] are possible in this regard. Since only real-valued wavenumbers are of interest in frequency-sweep analyses, polynomial approximations are more suitable for this work. In order to ensure an evenly distributed approximation error over the frequency range, a qth order polynomial

approximation of the form

$$\mathbf{H}(k) \approx \sum_{j=0}^{q} \mathbf{H}_j k^j = \mathbf{H}_0 + \mathbf{H}_1 k + \cdots + \mathbf{H}_q k^q \tag{9}$$

is used herein. For this, the system matrix $\mathbf{H}(k)$ is evaluated as usual by element-wise numerical integration at $s = q+1$ sample wavenumbers $k_1, \ldots, k_s$. These sample wavenumbers are chosen as the Chebyshev nodes in order to mitigate the effect of Runge's phenomenon.[34] Considering the interval $k \in [k_{\min}, k_{\max}]$, they are given by

$$k_j = 0.5(k_{\min} + k_{\max}) + 0.5(k_{\max} - k_{\min})\cos\frac{(2j-1)\pi}{2s}, \quad j = 1, \ldots, s. \tag{10}$$

With the system matrix samples $\mathbf{H}(k_1), \ldots, \mathbf{H}(k_s)$ at hand, the unknown coefficient matrices $\mathbf{H}_j$ of the polynomial approximation (9) can be determined by solving a sequence of linear systems of dimension s.

The approximation of the system matrix offers the additional advantage of requiring the set-up of $\mathbf{H}(k)$ only at a few sample frequencies. However, this advantage is lost if the numerical integration that goes along with the assembly of the right-hand side $\mathbf{b}$ is still performed at each frequency point of interest. Therefore, similar approximations are also employed for the right-hand side in order to preserve computational efficiency, i.e.

$$\mathbf{b}(k) \approx \sum_{j=0}^{q} \mathbf{b}_j k^j = \mathbf{b}_0 + \mathbf{b}_1 k + \cdots + \mathbf{b}_q k^q. \tag{11}$$

In contrast to the low-rank factorizations given in Sec. 2.2, the error introduced by the polynomial frequency approximations cannot be determined *a priori*. The error is mainly driven by the extent of the wavenumber interval $k_{\max} - k_{\min}$ on the one side and the chosen polynomial order on the other side. Assuming an evenly distributed error over the frequency range, an *a posteriori* evaluation of the error at a frequency between two neighboring samples could provide an estimation for an upper bound. The numerical examples in Sec. 3 give further insights in this regard.

2.3. *Algorithms for low-rank iteration schemes*

The nonsymmetric linear systems arising from acoustic BEM are usually addressed by iterative solvers based on Krylov subspace methods. Regarding multi-frequency problems, these iterative solvers are usually employed successively for each frequency. The overall computational effort is associated with the total number of matrix vector multiplications adding up over all iterations and frequency points. In contrast, the implementations in this paper seek for a simultaneous solution for the whole frequency range. Low-rank factorizations in conjunction with a frequency approximation of the BE matrix allow to replace the matrix vector multiplications by a single operation given by Eq. (5) covering all frequency points. Moreover, the algorithms in this paper are nonstandard in the sense that the iterates are matrices instead of vectors.

Algorithm 1 Low-rank BiCGstab

input
- linear operator $\boldsymbol{\mathcal{H}} : \mathbb{C}^{n\times m} \to \mathbb{C}^{n\times m}$ as given in Eq. (5)
- truncation operator $\boldsymbol{\mathcal{T}} : \mathbb{C}^{n\times m} \to \mathbb{C}^{n\times m}$ as described in Sec. 2.2
- relative error for the low-rank approximation $\epsilon_{\mathcal{T}}$
- relative residual tolerance ϵ_{tol}
- right-hand side $\mathbf{B} \in \mathbb{C}^{n\times m}$

set
- $\mathbf{B} := \boldsymbol{\mathcal{T}}(\mathbf{B})$
- initial guess $\mathbf{P}_0 := \mathbf{0}$, $\mathbf{R}_0 := \mathbf{B}$
- $\rho_0 := \langle \mathbf{B}, \mathbf{R}_0 \rangle$
- $\mathbf{Y}_0 := \mathbf{R}_0$
- $\mathbf{W}_0 := \boldsymbol{\mathcal{H}}(\mathbf{Y}_0)$, $\mathbf{W}_0 := \boldsymbol{\mathcal{T}}(\mathbf{W}_0)$
- $j := 0$

while $\|\mathbf{R}_j\|_{\text{F}}/\|\mathbf{B}\|_{\text{F}} > \epsilon_{\text{tol}}$ **do**
- $\alpha_j := \rho_j / \langle \mathbf{B}, \mathbf{W}_j \rangle$, breakdown if $\langle \mathbf{B}, \mathbf{W}_j \rangle = 0$
- $\mathbf{S}_j := \mathbf{R}_j - \alpha_j \mathbf{W}_j$, $\mathbf{S}_j := \boldsymbol{\mathcal{T}}(\mathbf{S}_j)$
- **if** $\|\mathbf{S}_j\|_{\text{F}}/\|\mathbf{B}\|_{\text{F}} < \epsilon_{\text{tol}}$ **then**
  - $\mathbf{P} := \mathbf{P}_j + \alpha_j \mathbf{Y}_j$, **return**
- $\mathbf{T}_j := \boldsymbol{\mathcal{H}}(\mathbf{S}_j)$, $\mathbf{T}_j := \boldsymbol{\mathcal{T}}(\mathbf{T}_j)$
- $\xi_j := \langle \mathbf{T}_j, \mathbf{S}_j \rangle / \langle \mathbf{T}_j, \mathbf{T}_j \rangle$
- $\mathbf{P}_{j+1} := \mathbf{P} + \alpha_j \mathbf{Y}_j + \xi_j \mathbf{S}_j$
- $\mathbf{R}_{j+1} := \mathbf{S}_j - \xi_j \mathbf{T}_j$, $\mathbf{R}_{j+1} := \boldsymbol{\mathcal{T}}(\mathbf{R}_{j+1})$
- $\rho_{j+1} := \langle \mathbf{B}, \mathbf{R}_{j+1} \rangle$
- $\beta_j := (\rho_{j+1}\alpha_j)/(\rho_j \xi_j)$, breakdown if $\rho_j \xi_j = 0$
- $\mathbf{Y}_{j+1} := \mathbf{R}_{j+1} + \beta_j(\mathbf{Y}_j - \xi_j \mathbf{W}_j)$, $\mathbf{Y}_{j+1} := \boldsymbol{\mathcal{T}}(\mathbf{Y}_{j+1})$
- $\mathbf{W}_{j+1} := \boldsymbol{\mathcal{H}}(\mathbf{Y}_{j+1})$, $\mathbf{W}_{j+1} := \boldsymbol{\mathcal{T}}(\mathbf{W}_{j+1})$
- $j := j + 1$

output
- $\mathbf{P} \in \mathbb{C}^{n\times m}$ with $\|\boldsymbol{\mathcal{H}}(\mathbf{P}) - \mathbf{B}\|_{\text{F}}/\|\mathbf{B}\|_{\text{F}} \leq \epsilon_{\text{tol}}$

The incorporation of the low-rank format into BiCGstab[30,35] is given in Algorithm 1. In there, inner products of two matrices $\langle \mathbf{X}, \mathbf{Y} \rangle$ need to be evaluated, which can be performed economically, if $\mathbf{X} = \mathbf{U}_{\mathbf{X}} \mathbf{V}_{\mathbf{X}}^{\text{H}}$ and $\mathbf{Y} = \mathbf{U}_{\mathbf{Y}} \mathbf{V}_{\mathbf{Y}}^{\text{H}}$ are available in the low-rank format as

$$\langle \mathbf{X}, \mathbf{Y} \rangle = \text{trace}(\mathbf{X}^{\text{H}} \mathbf{Y}) = \text{trace}((\mathbf{V}_{\mathbf{Y}}^{\text{H}} \mathbf{V}_{\mathbf{X}})(\mathbf{U}_{\mathbf{X}}^{\text{H}} \mathbf{U}_{\mathbf{Y}})). \tag{12}$$

A restarted low-rank GMRes[31,36,37] is summarized in Algorithm 2. In there, a new basis vector $\mathbf{S}_{k+1}$ of the subspace $\text{span}(\mathbf{S}_1, \ldots, \mathbf{S}_d)$ is obtained by applying the system matrix to the basis vector $\mathbf{S}_k$ of the previous iteration, which would lead to a rank increase over the iterations. In order to avoid this, the basis vectors are truncated as described in Sec. 2.2, although thereby their orthogonality is lost. Consequently, cheap estimations of both, the

Algorithm 2 Restarted low-rank GMRes

input
  linear operator $\boldsymbol{\mathcal{H}} : \mathbb{C}^{n\times m} \to \mathbb{C}^{n\times m}$ as given in Eq. (5)
  truncation operator $\boldsymbol{\mathcal{T}} : \mathbb{C}^{n\times m} \to \mathbb{C}^{n\times m}$ as described in Sec. 2.2
  relative error for the low-rank approximation $\epsilon_{\mathcal{T}}$
  relative residual tolerance ϵ_{tol}
  dimension of the Krylov subspace d
  right-hand side $\mathbf{B} \in \mathbb{C}^{n\times m}$
set
  initial guess $\mathbf{P}_0 \coloneqq \mathbf{0}$, $\mathbf{R}_0 \coloneqq \mathbf{B}$
  $j \coloneqq 0$
while $\|\mathbf{R}_j\|_{\text{F}}/\|\mathbf{B}\|_{\text{F}} > \epsilon_{\text{tol}}$ **do**
  $\tilde{\mathbf{S}}_1 \coloneqq \mathbf{R}_j$, $\tilde{\mathbf{S}}_1 \coloneqq \boldsymbol{\mathcal{T}}(\tilde{\mathbf{S}}_1)$
  $\mathbf{S}_1 \coloneqq \tilde{\mathbf{S}}_1/\|\tilde{\mathbf{S}}_1\|_2$
  for $k = 1,...,d$ **do**
    $\mathbf{W}_k \coloneqq \boldsymbol{\mathcal{H}}(\mathbf{S}_k)$, $\mathbf{W}_k \coloneqq \boldsymbol{\mathcal{T}}(\mathbf{W}_k)$
    Solve $[\langle \mathbf{S}_p, \mathbf{S}_q\rangle]_{p,q=1}^{k}\alpha = [\langle \mathbf{S}_p, \mathbf{W}_k\rangle]_{p=1}^{k}$ for $\alpha \in \mathbb{C}^{k\times 1}$
    $\tilde{\mathbf{S}}_{k+1} \coloneqq \mathbf{W}_k - \sum_{i=1}^{k} \alpha_i \mathbf{S}_i$, $\tilde{\mathbf{S}}_{k+1} \coloneqq \boldsymbol{\mathcal{T}}(\tilde{\mathbf{S}}_{k+1})$
    $\mathbf{S}_{k+1} \coloneqq \tilde{\mathbf{S}}_{k+1}/\|\tilde{\mathbf{S}}_{k+1}\|_2$
  Solve $[\langle \mathbf{W}_p, \mathbf{W}_q\rangle]_{p,q=1}^{d}\beta = [\langle \mathbf{W}_p, \mathbf{R}_j\rangle]_{p=1}^{d}$ for $\beta \in \mathbb{C}^{d\times 1}$
  $\mathbf{P}_{j+1} \coloneqq \mathbf{P}_j + \sum_{i=1}^{d} \beta_i \mathbf{S}_i$, $\mathbf{P}_{j+1} \coloneqq \boldsymbol{\mathcal{T}}(\mathbf{P}_{j+1})$
  $\mathbf{R}_{j+1} \coloneqq \mathbf{B} - \boldsymbol{\mathcal{H}}(\mathbf{P}_{j+1})$
  $j \coloneqq j + 1$
output
  $\mathbf{P} \in \mathbb{C}^{n\times m}$ with $\|\boldsymbol{\mathcal{H}}(\mathbf{P}) - \mathbf{B}\|_{\text{F}}/\|\mathbf{B}\|_{\text{F}} \leq \epsilon_{\text{tol}}$

residual and the required subspace dimension d inside the inner loop of Algorithm 2 are no longer possible. Instead, d is assumed to be predefined in this paper. An elaborate discussion on the implications of approximate basis vectors in GMRes can be found in the paper by Ballani and Grasedyck.[31]

2.4. *Some remarks on preconditioning*

A preconditioner $\boldsymbol{\mathcal{M}} : \mathbb{C}^{n\times m} \to \mathbb{C}^{n\times m}$ could be employed in order to accelerate the convergence of the solution. Ideally, it should be defined such that $\boldsymbol{\mathcal{M}}^{-1}$ admits an economic application to matrices in the low-rank format and reduces the condition number in the whole frequency range. Incorporations of preconditioners in low-rank versions of both BiCGstab and GMRes are described in the literature for special cases such as linear parameter dependence[30] and block diagonal systems,[37] but they are not applicable in the herein presented case of polynomially approximated frequency dependency. An alternative way is to apply well-known preconditioners for single frequency BE matrices[38,39] to individual columns of

P before truncation. However, the choice of suitable frequency samples for preconditioning is indeed an intricate task and would require *a priori* estimation of condition numbers. Preliminary experiments with explicitly preconditioning at (or even omitting) the frequency samples associated with high condition numbers (typically those in the vicinity of eigenfrequencies) only marginally improved the convergence in the tested cases. For the remainder of the paper, preconditioning is neglected in Algorithms 1 and 2.

3. Numerical Examples

The key concepts of the proposed scheme include a polynomial approximation of the system matrix, low-rank factorizations and their incorporation into iterative solvers. These concepts are verified each based on an interior duct problem in Sec. 3.1. An exterior scattering problem is analyzed in Sec. 3.2 and the computational times are compared to those of a conventional frequency-wise strategy.

3.1. *Two-dimensional duct with reflecting and absorbing boundary conditions*

A closed, two-dimensional duct of length $l = 3.4\,\mathrm{m}$ and width $w = 0.2\,\mathrm{m}$ is considered, as shown in Fig. 1. A plane sound wave is excited harmonically due to a particle velocity $v_0 = 1\,\mathrm{mm/s}$ at $x = 0$ and propagates through air with a density of $\rho = 1.3\,\mathrm{kg/m^3}$ and speed of sound of $c = 340\,\mathrm{m}/s$. The example is studied in the frequency range from 421 to 520 Hz in steps of $\Delta f = 1\,\mathrm{Hz}$. Hence, using state-of-the-art solution schemes, $m = 100$ linear systems need to be solved. At the right end $x = l$, two different boundary conditions are considered. First, an admittance boundary condition with $Y(l) = 1/\rho c$ is used, which results in full absorption of the wave at the outlet $x = l$. This will be referred to as the condition (I). Second, sound hard boundary conditions $Y(l) = 0$ are employed, denoted as condition (II). They lead to a full reflection of the wave, and hence, standing waves emerge at the resonance frequencies of 450 and 500 Hz. Similar models comprising plane sound waves inside two- and three-dimensional ducts are widely used as benchmark problems in computational acoustics[40] and extensive studies on associated discretization errors with respect to mesh sizes and element types are available in the literature.[41,42]

A total of 32 one-dimensional isoparametric elements of quadratic order resulting in $n = 64$ DOFs are employed for discretizing the sound pressure on the boundary of the duct, where the edges parallel to the direction of wave propagation accommodate 15 elements, respectively. At 500 Hz, this corresponds to a ratio of three elements per wavelength.

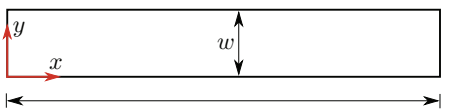

Fig. 1. Schematic of the air-filled two-dimensional duct.

3.1.1. *Assessment of the frequency approximations*

Before studying the characteristics of the proposed iterative scheme, the applicability of the underlying approximations is assessed in what follows. This section is concerned with errors associated with the frequency approximations excluding the effects of low-rank approximations and iterative solvers.

Polynomial frequency approximations of orders $q = 3, \ldots, 6$ are computed for the system matrix $\mathbf{H}(k) \in \mathbb{C}^{64\times64}$. The corresponding right-hand side vectors $\mathbf{b}(k) \in \mathbb{C}^{64\times1}$ are also approximated across the frequency range using the same sample frequencies. This is done in order to achieve efficiency of the algorithm as discussed in Sec. 2.1. The approximations of $\mathbf{H}(k)$ and $\mathbf{b}(k)$ are then evaluated at the wavenumbers $k_1, \ldots, k_m$ and the m linear systems are solved individually using a direct solver. The real parts of the resultant sound pressure solutions at the corner node $(x, y) = (0, 0)$ are displayed in Figs. 2 and 3. Qualitatively, the results accord well with the conventional solutions that are obtained by setting up the system matrices and right-hand sides for each wavenumber $k_1, \ldots, k_m$. This also applies to all other positions in the duct, as well as the imaginary parts of the solutions. The graphs in Fig. 3 display the sound pressure solution for the condition (II). As expected, resonances occur at 450 and 500 Hz, respectively, and relatively large deviations are observed around them. However, considering that the resonance frequencies and associated amplitudes are generally

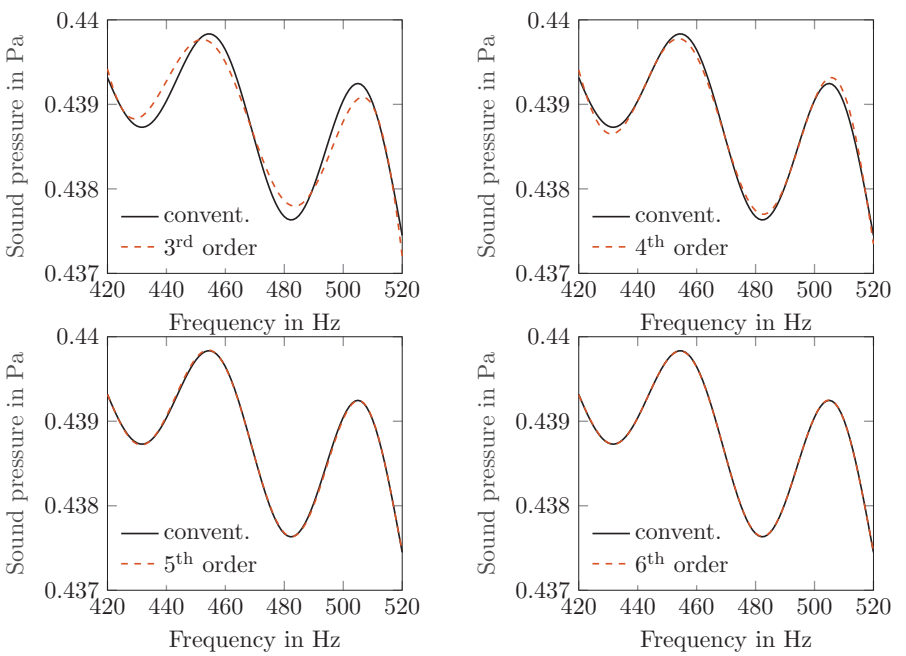

Fig. 2. Real parts of the sound pressure solutions at the corner $(x, y) = (0, 0)$ in the duct with absorbing condition (I) over frequency. Comparison of conventionally obtained solutions and solutions obtained by using different orders of polynomial approximations for right-hand sides and system matrices.

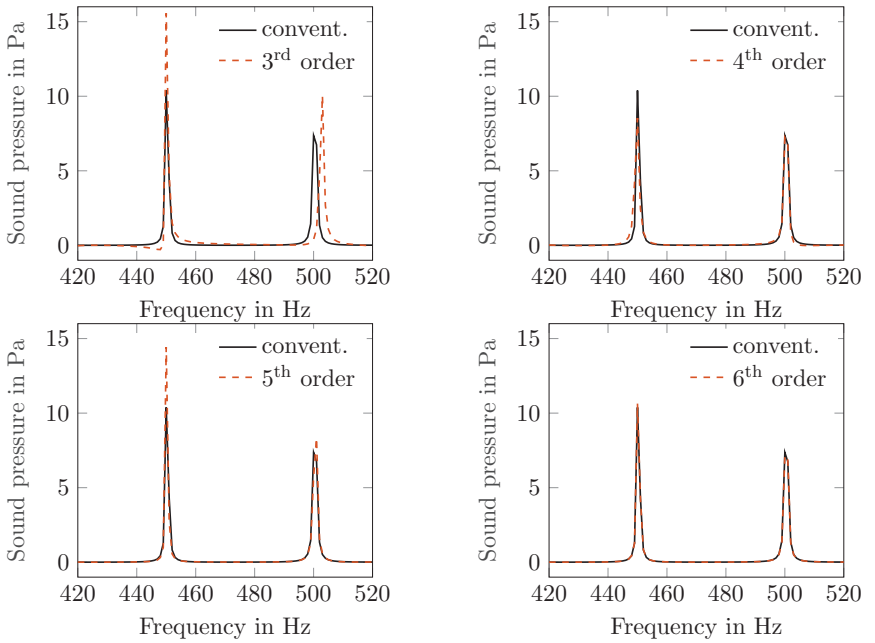

Fig. 3. Real parts of the sound pressure solutions at the corner $(x, y) = (0, 0)$ in the duct with sound hard condition (II) over frequency. Comparison of conventionally obtained solutions and solutions obtained by using different orders of polynomial approximations for right-hand sides and system matrices.

subject to uncertainties such as the extent of damping, the overall accuracy achieved with the frequency approximations is acceptable with regard to most engineering applications.

In addition to the qualitative comparisons shown in Figs. 2 and 3, the errors introduced to the system matrices are quantified using the Frobenius norm, i.e.

$$\epsilon_{\text{rel,H}} = \frac{\|\sum_{j=0}^{q} \mathbf{H}_j k^j - \mathbf{H}(k)\|_{\text{F}}}{\|\mathbf{H}(k)\|_{\text{F}}}, \quad k = k_1, \ldots, k_m, \tag{13}$$

and they are given in Fig. 4. The errors are smallest around the sample frequencies and are largest between two sample frequencies. As expected, higher polynomial orders provide better approximations. The relative errors in the corresponding sound pressure solutions are depicted in Fig. 5. They are determined for each frequency in the Euclidean norm from

$$\epsilon_{\text{rel,p}} = \frac{\|\tilde{\mathbf{p}} - \mathbf{p}\|_2}{\|\mathbf{p}\|_2}, \quad \tilde{\mathbf{p}} = \tilde{\mathbf{p}}_1, \ldots, \tilde{\mathbf{p}}_m, \quad \mathbf{p} = \mathbf{p}_1, \ldots, \mathbf{p}_m, \tag{14}$$

where $\tilde{\mathbf{p}}$ is obtained using the approximations in Eqs. (9) and (11). The sound pressure errors in condition (I) show similar distributions as the corresponding matrix errors in Fig. 4 providing minima at the Chebyshev nodes and upper bounds for each approximation, respectively. For example, a 6th-order matrix approximation subjects the sound pressure solution to an error of $\epsilon_{\text{rel,p}} < 10^{-3}$ in the considered frequency range. However, in condition (II), significantly higher errors are encountered in the vicinity of the eigenfrequencies. They stem from the ill-conditioned matrix $\mathbf{H}(k)$ at the resonances and thus a high sensitivity

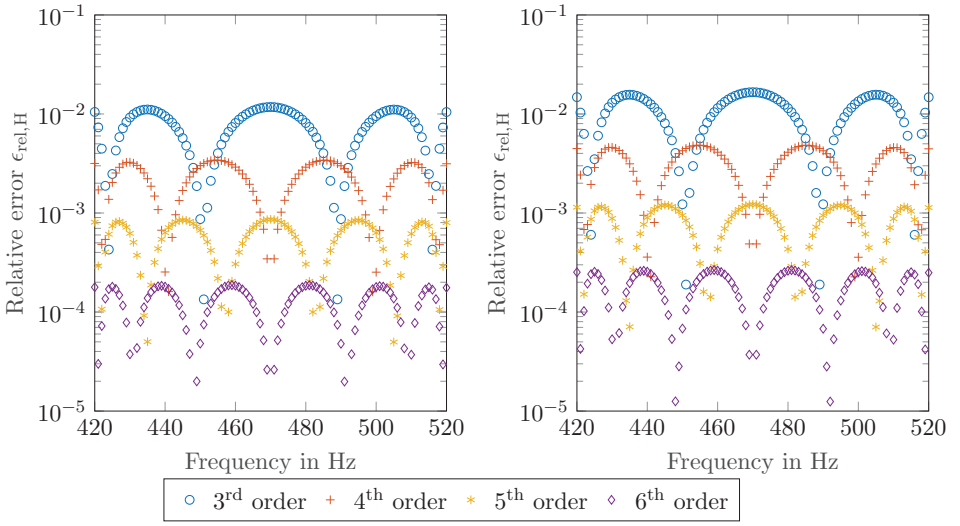

Fig. 4. Relative errors in the Frobenius norm of polynomial approximations of the system matrices. Absorbing condition (I) on the left and sound hard condition (II) on the right.

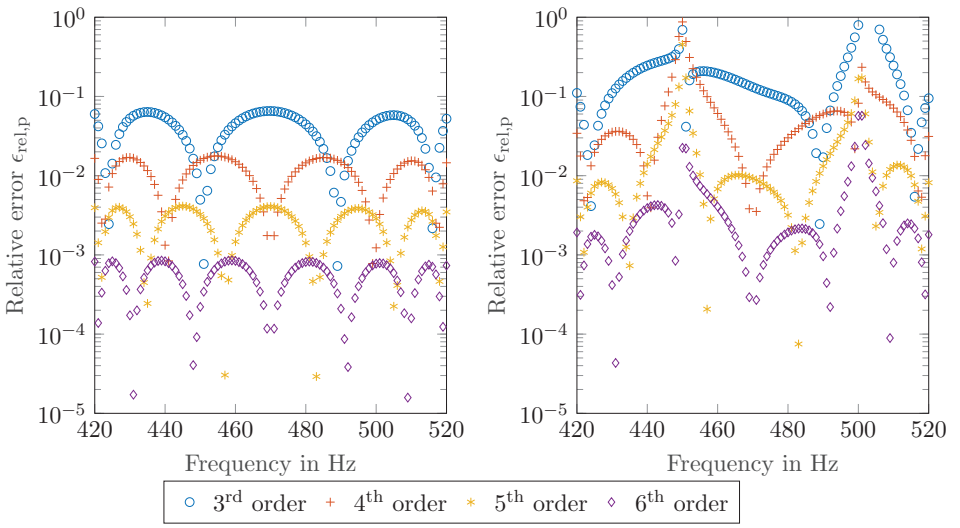

Fig. 5. Relative errors in the Euclidean norm of the sound pressure solutions obtained using polynomial approximations of the right-hand sides and system matrices. Absorbing condition (I) on the left and sound hard condition (II) on the right.

of the solution accuracy with respect to approximation errors. Relatively small errors in the system matrices and right-hand sides give rise to large deviations in amplitudes as well as to frequency shifts at the resonances. Both can be seen in Fig. 3. However, as already mentioned, the qualitative accordance and the overall accuracy can be judged to be acceptable for both conditions (I) and (II).

While the results in Figs. 2 to 5 indicate an improvement in accuracy with increasing polynomial orders, it has to be noted that the polynomial order cannot be chosen arbitrarily high. In this example, orders greater than six induce numerical instabilities due to round-off errors in the coefficient matrices of Eq. (9).

3.1.2. *Assessment of the low-rank factorizations*

Beside frequency approximations of $\mathbf{H}(k)$ and $\mathbf{b}(k)$, a low-rank factorization accounts for a second approximation underlying the proposed iterative scheme. For the efficiency of the scheme, it is crucial that the solution matrix $\mathbf{P}$ and the right-hand side $\mathbf{B}$ both admit a low-rank factorization, i.e. they can be well approximated by only taking a small number of singular values and singular vectors into account. This property is assessed in this section on the example of the duct problem. The admissibility of low-rank approximations is studied in an isolated manner as well as in combination with the polynomial frequency approximations. The effect of iterative solvers is excluded altogether.

Figure 6 shows the singular values of both $\mathbf{B}$ and $\mathbf{P}$ for conditions (I) and (II) when obtained conventionally by numerical integration for each frequency as well as by means of the frequency approximations described in Sec. 2.1. As discussed in Sec. 2.2, the conventionally obtained matrices exhibit an exponential singular value decay. However, this does not hold when using polynomial frequency approximations of $\mathbf{H}(k)$ and $\mathbf{b}(k)$. Considering a qth order approximation of the right-hand side $\mathbf{B} = [\mathbf{b}(k_1), \ldots, \mathbf{b}(k_m)]$, its column vectors are linear combinations of $q+1$ coefficient vectors, c.f. Eq. (11). Hence, the polynomial approximation of $\mathbf{B}$ is of rank $(\mathbf{B}) \leq q+1$. For example, Fig. 6 indicates that the 6th-order approximation of $\mathbf{B}$ yields a good accordance in the first seven singular values. Note that the smaller singular values do not vanish due to finite arithmetic accuracy. The same issue can be observed for the first seven singular values of the resulting solution matrices $\mathbf{P}$. They agree well with those of the conventionally obtained matrices. However, using polynomial approximations for $\mathbf{H}(k)$ and $\mathbf{b}(k)$, the smaller singular values of $\mathbf{P}$ do no longer exhibit an

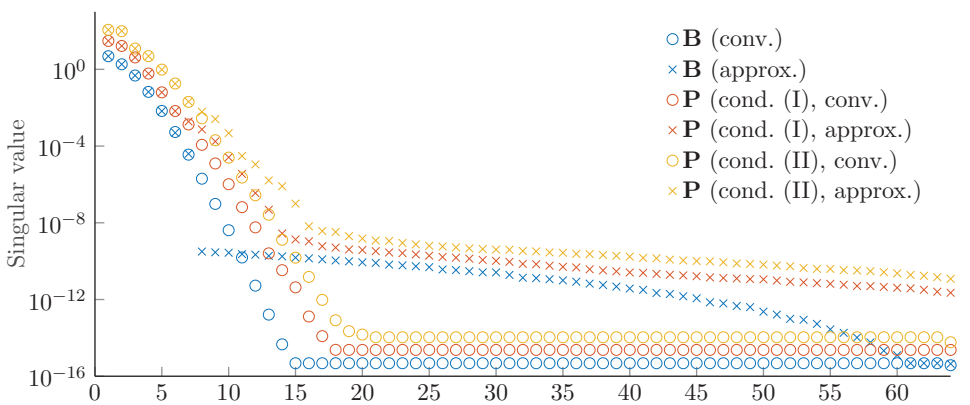

Fig. 6. Singular values of right-hand sides $\mathbf{B}$ and solutions $\mathbf{P}$ for conditions (I) and (II) for conventionally obtained matrices and using 6th-order polynomial approximations.

exponential decay. These considerations are essential when choosing the relative error $\epsilon_{\mathcal{T}}$ for the low-rank approximation in Algorithms 1 and 2.

The ranks of $\mathbf{B}$ and $\mathbf{P}$ after computing SVDs and performing truncations with different relative errors $\epsilon_{\mathcal{T}}$ are given in Table 1. As expected, the ranks are slightly higher when using polynomial approximations, in particular with regard to higher accuracies $\epsilon_{\mathcal{T}}$. Nonetheless, the ranks are still considerably smaller than m and n, and hence, the products in Algorithms 1 and 2 can be efficiently computed by making use of the low-rank format.

3.1.3. *Convergence behaviors of the low-rank iteration schemes*

Having assessed the implications of polynomial frequency approximations and low-rank factorizations, the characteristics of the iterative schemes incorporating these approximations are examined hereinafter. The convergence of the relative residuals $\|\mathbf{R}\|_{\mathrm{F}}/\|\mathbf{B}\|_{\mathrm{F}}$ for both, the absorbing (I) and the sound hard condition (II), are shown in Fig. 7 for GMRes. A restart parameter of $d = 5$ is used in this example and the indicated numbers of iterations in Fig. 7 refer to the cumulative repetitions of the inner loop of Algorithm 2, that is d times the number of restarts. The residuals decrease monotonically over the course of the iterations. Initially, the rate of convergence is independent of the accuracy of the low-rank approximation $\epsilon_{\mathcal{T}}$, but the truncations cause early stagnation of the method at residuals depending on the chosen value for $\epsilon_{\mathcal{T}}$. However, the convergence behavior up to the point of reaching the respective final accuracy is not deteriorated. While in the absorbing condition (I), convergence is reached rather quickly, the convergence rate in the sound hard condition (II) is much slower due to the resonances and associated high condition numbers of $\mathbf{H}(k)$.

Similar convergence plots are given in Fig. 8 for BiCGstab. In contrast to GMRes, the residuals do not decrease monotonically over the course of the iterations. In condition (I), different accuracies of the low-rank approximation $\epsilon_{\mathcal{T}}$ do not have a significant influence on the convergence, while in condition (II), higher accuracies are associated with faster convergence. In this example, the residuals decrease without being restricted by the low-rank approximations. However, note that in case of evaluating the residual explicitly by

Table 1. Ranks of right-hand sides $\mathbf{B}$ and solutions $\mathbf{P}$ for conditions (I) and (II) after SVD and truncation with relative errors $\epsilon_{\mathcal{T}}$ for conventionally obtained matrices and using 6th-order polynomial approximations.

$\epsilon_{\mathcal{T}}$	10^{-4}	10^{-6}	10^{-8}
$\mathbf{B}$ (conv.)	6	7	9
$\mathbf{B}$ (approx.)	5	7	7
$\mathbf{P}$ (cond. (I), conv.)	6	8	10
$\mathbf{P}$ (cond. (I), approx.)	6	9	12
$\mathbf{P}$ (cond. (II), conv.)	7	9	11
$\mathbf{P}$ (cond. (II), approx.)	7	10	13

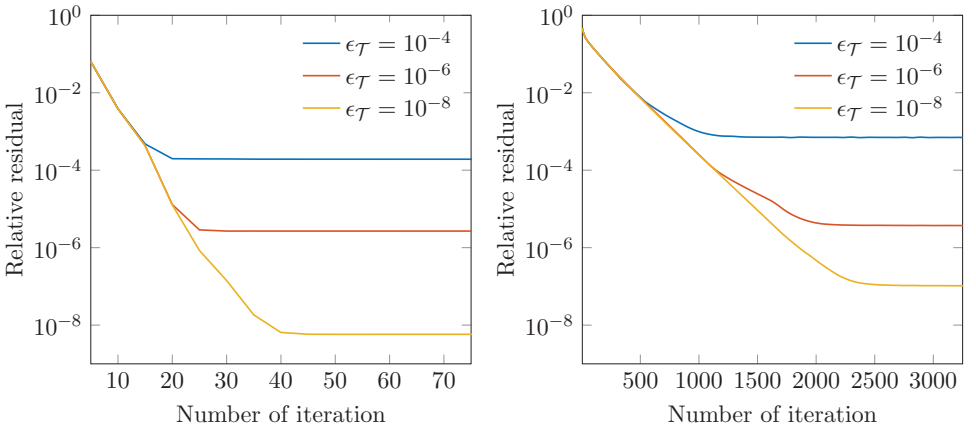

Fig. 7. Convergence behavior of low-rank GMRes ($d = 5$) with different relative errors for the low-rank approximation $\epsilon_{\mathcal{T}}$. Absorbing condition (I) on the left and sound hard condition (II) on the right. The number of iterations refers to d times the number of restarts.

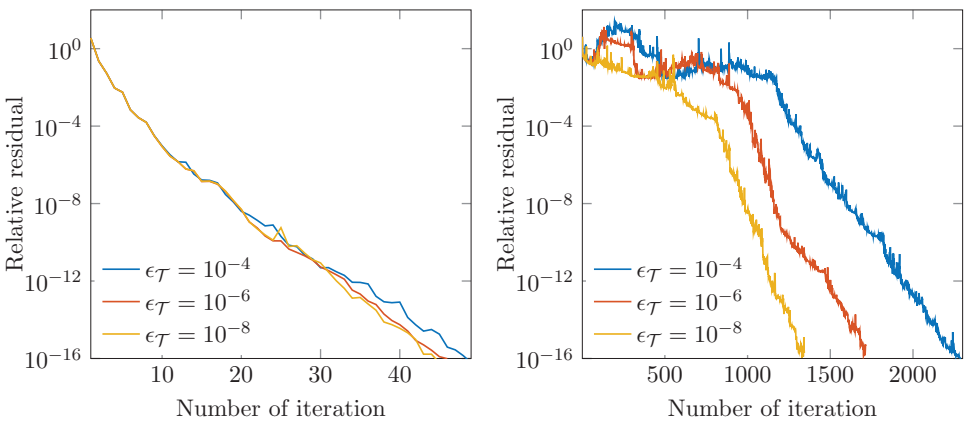

Fig. 8. Convergence behavior of low-rank BiCGstab with different relative errors for the low-rank approximation $\epsilon_{\mathcal{T}}$. Absorbing condition (I) on the left and sound hard condition (II) on the right.

$\mathbf{R}_{j+1} := \mathbf{B} - \boldsymbol{\mathcal{H}}(\mathbf{P}_{j+1})$ instead of the using the recursion formula in line 22 of Algorithm 1, the residual stagnates depending on the chosen value for $\epsilon_{\mathcal{T}}$ similarly to GMRes.

The overall computational time is mainly driven by the efforts associated with the evaluation of matrix products and the computation of the low-rank factorizations within each iteration as well as the total number of iterations. While low numerical ranks clearly reduce the efforts for evaluating matrix products, the numerical experiments indicate that they can be detrimental in terms of the rate of convergence, i.e. the number of iterations. Therefore, omitting some of the truncations in the loop of Algorithm 1 could be beneficial regarding the overall computational time. The optimal trade-off between fast evaluations of matrix products by low numerical ranks on the one side and the additional effort for the SVDs

as well as a possible increase in the number of iterations on the other side is certainly problem-dependent. Further studies are required to gain confidence in this regard.

As a final remark, it should be noted that though the solution and right-hand side both admit low-rank approximations as confirmed by Table 1, the ranks of intermediate matrices could temporarily grow larger in the course of the iterations. This can be avoided by truncating the respective matrices to a fixed rank, however thereby sacrificing information on the introduced numerical error. Preliminary numerical experiments indicate that this can be feasible in GMRes, since after all, the subspaces are discarded at the restarts.

3.2. *Plane wave scattering on a rigid sphere*

The second example involves a rigid sphere with a radius of 5 m submerged in water with a density of $\rho = 1000\,\mathrm{kg/m^3}$ and speed of sound of $c = 1500\,\mathrm{m}/s$. The sphere is subject to an infinite incident plane wave with an amplitude of $p_0 = 1\,\mathrm{Pa}$. Only scattering is considered and hence, the right-hand side in Eq. (1) only comprises the incident sound pressure vector $\mathbf{p}_\mathrm{i}$. The problem is analyzed in the frequency range from 10 to 130 Hz in frequency steps of $\Delta f = 1\,\mathrm{Hz}$, i.e. $m = 121$. A treatment for irregular frequencies is not required, since the first eigenfrequency of the interior Dirichlet problem is approximately 148 Hz.

The acoustic field is discretized by 864 quadrilateral boundary elements with bi-quadratic geometry approximation and discontinuous bi-linear sound pressure approximation. This corresponds to 12 elements on a $\pi/2$ arc and a total of $n = 3456\,\mathrm{DOFs}$.

First, the problem is addressed in conventional manner by solving each of the $m = 121$ linear systems independently by standard GMRes without restarts. For this, the built-in MATLAB function `gmres` is employed with a tolerance of $\epsilon_\mathrm{tol} = 10^{-6}$ for the relative residual. A cumulative number of 577 iterations is required adding up to a total wall clock time of 10.4 s. Note that this does not include the time for setting up the BE matrices but only the actual solution of the linear systems. The evaluation of a single matrix vector product takes approximately 0.006 s.

Second, the low-rank BiCGstab method described in Algorithm 1 is applied for a simultaneous frequency range solution. The BE matrix is approximated by a polynomial of order $q = 6$. The tolerance for the low-rank truncation is set to $\epsilon_\mathcal{T} = 10^{-6}$, which yields a rank of $r = 7$ for the solution matrix $\mathbf{P}$ after convergence. Low-rank BiCGstab requires 16 iterations to reach a relative residual of $\epsilon_\mathrm{tol} = 10^{-6}$ corresponding to a wall clock time of 4.3 s. Higher values for $\epsilon_\mathcal{T}$ of course result in higher ranks but do hardly affect the wall clock time. The relative difference in the sound pressure solution is $\|\mathbf{P}_\mathrm{conv} - \mathbf{P}\|_\mathrm{F}/\|\mathbf{P}_\mathrm{conv}\|_\mathrm{F} = 3.8 \cdot 10^{-4}$, where $\mathbf{P}_\mathrm{conv}$ denotes the solution matrix obtained by the above-described conventional approach. The evaluation of the operator in Eq. (5) takes approximately 0.07 s.

Third, the problem is addressed by the low-rank GMRes method described in Algorithm 2, using the same parameters as above, i.e. $q = 6$, $\epsilon_\mathcal{T} = 10^{-6}$ and $\epsilon_\mathrm{tol} = 10^{-6}$. The restart parameter is set to $d = 5$. Again, the rank of $\mathbf{P}$ after convergence is $r = 7$. Low-rank GMRes takes six outer iterations and a wall clock time of 5.4 s for the frequency range solution.

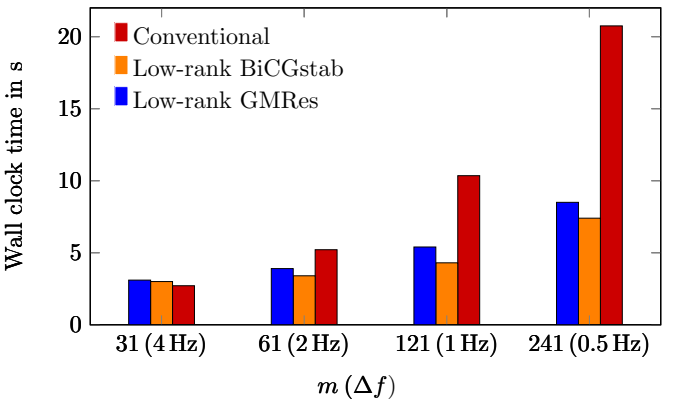

Fig. 9. Comparison between conventional strategy and the low-rank versions of BiCGstab and GMRes. Wall clock times for the solution of the scattering problem in the frequency range from 10 to 130 Hz using different resolutions (i.e. frequency steps Δf).

In summary, the low-rank versions of BiCGstab and GMRes have reduced the computational time for solving the given scattering problem by 59 % and 48 %, respectively. But as with all multi-frequency solvers, the success of the proposed low-rank schemes depends on the desired frequency resolution. This issue is illustrated in Fig. 9, which shows the solution time of the scattering problem for different frequency resolutions. While the solution time of the conventional approach increases proportionally with the number of frequency samples m, this rate is much smaller when using the low-rank schemes. On the other hand, in this example, the conventional strategy is more efficient when the frequency steps go beyond $\Delta f = 2\,\text{Hz}$, which corresponds to $m = 61$.

4. Conclusions and Future Work

A low-rank iteration scheme has been proposed for the frequency range solution of acoustic problems with BEM. It is based on a polynomial frequency approximation of BE equations and on low-rank factorizations of intermediate matrices. Combining both concepts enables efficient evaluations of matrix vector products, and their incorporation into BiCGstab and GMRes has been presented. The method has been applied to an interior duct problem subject to absorbing and to sound hard boundary conditions in order to provide a proof of concept. The implications of the underlying approximation have been assessed systematically and the convergence behaviors of low-rank versions of BiCGstab and GMRes have been studied. Further, an exterior scattering problem has been analyzed, and the computational times have been compared to those of a conventional frequency-wise strategy. As expected, the benefit of the proposed low-rank schemes increases with the chosen frequency resolution. Hence, the common issue of oversampling the frequency range has less of an impact on the computational time.

Acceptable accuracies have been achieved in the whole frequency range using polynomial frequency approximations. However, the size of the frequency interval is limited since

overly large intervals would require high polynomial orders possibly resulting in numerical instabilities. Piece-wise polynomial approximations of lower orders could address this issue. As an alternative, the discrete empirical interpolation method could be used for improving the frequency approximation.[45]

The numerical examples have also confirmed the admissibility of truncating solution and right-hand side matrices to low numerical ranks. Clearly, this is the key concept of the method since low numerical ranks are crucial for efficient evaluation of products in the course of the iterations. For this, SVDs need to be computed repeatedly accounting for a major share in the overall computational time. While a standard algorithm based on bidiagonalization has been employed in this work, more efficient strategies are available, such as the computation of a subset of singular values[43] or randomized SVD.[44] Their incorporation into the proposed low-rank iteration schemes is certainly a task for future research.

Regarding the behaviors of the low-rank-based iterative schemes, BiCGstab and GMRes have both shown convergence. Although the basis vectors spanning the subspace are not orthogonal in low-rank GMRes, it has provided monotone decrease of the residual until reaching the final accuracy in the considered example. While in the traveling wave and the exterior scattering problem, relatively high rates of convergence have been obtained, a considerably large number of iterations was required to achieve convergence in the duct problem with sound hard boundary conditions due to the emerging resonances.

The development of efficient preconditioning is therefore crucial in order to extend the applicability of the method to actual technical and scientific problems. A preconditioner should be defined such that it first allows for an economic application to matrices in the low-rank format and second decreases the condition number uniformly over the whole frequency range. Several approaches for the preconditioning of parametrized linear systems exist in the literature,[46,47] however incorporating them into low-rank iteration schemes is an ongoing challenge.

The main purpose of this paper is to provide a proof of concept and to initiate further research on the applicability of low-rank solvers in the field of computational acoustics. Though only frequency-dependent BE matrices have been considered here, the concept can be straightforwardly applied to other parametrized linear systems as those originating from vibroacoustic optimization problems and uncertainty quantification. Moreover, multiple parameter dependence can be handled by making use of the low-rank tensor format.

In this paper, academic problems with relatively small numbers of DOFs have been considered with the aim to verify the underlying approximations of the method. Examining larger problems and comparing the performance to other multi-frequency strategies with regard to computational efficiency are tasks for future research. The high complexity and memory requirements associated with fully populated BE matrices have given rise to several fast algorithms such as hierarchical matrices.[23] They provide reduced memory requirements and fast evaluation of matrix operations and hence, enable the treatment of large problems with BEM. Their incorporation into the proposed low-rank iteration scheme is vital in order to avoid the storage of several fully populated coefficient matrices.

Acknowledgments

The work of S. K. Baydoun was supported by the German Research Foundation (DFG project MA 2395/15-2) in the context of the priority program 1897 "Calm, Smooth and Smart - Novel Approaches for Influencing Vibrations by Means of Deliberately Introduced Dissipation."

References

1. T. Wu (ed.), *Boundary Element Acoustics: Fundamentals and Computer Codes* (WIT Press, Southampton, 2000).
2. O. von Estorff (ed.), *Boundary Elements in Acoustics: Advances and Applications* (WIT Press, Southampton, 2000).
3. S. Kirkup, The boundary element method in acoustics: A survey, *Appl. Sci.* **9** (2019) 1642.
4. K.-J. Bathe, *Finite Element Procedures* (Prentice Hall, Englewood Cliffs, New Jersey, 1996).
5. I. Harari and T. J. R. Hughes, A cost comparison of boundary element and finite element methods for problems of time-harmonic acoustics, *Comput. Methods Appl. Mech. Eng.* **97** (1992) 77–102.
6. U. Hetmaniuk, R. Tezaur and C. Farhat, Review and assessment of interpolatory model order reduction methods for frequency response structural dynamics and acoustics problems, *Int. J. Numer. Methods Eng.* **90** (2012) 1636–1662.
7. M. Petyt, J. Lea and G. Koopmann, A finite element method for determining the acoustic modes of irregular shaped cavities, *J. Sound Vib.* **45** (1976) 495–502.
8. G. W. Benthien and H. A. Schenk, Structural–acoustic coupling, in *Boundary Element Methods in Acoustics*, eds. R. D. Ciskowski and C. A. Brebbia (Computational Mechanics Publications, Elsevier Applied Science, 1991).
9. S. M. Kirkup and D. J. Henwood, Methods for speeding up the boundary element solutions of acoustic radiation problems, *J. Vib. Acoust.* **144** (1992) 347–380.
10. T. W. Wu, W. L. Li and A. F. Seybert, An efficient boundary element algorithm for multi-frequency acoustical analysis, *J. Acoust. Soc. Am.* **94** (1993) 447–452.
11. S. M. Kirkup and S. Amini, Solution of the Helmholtz eigenvalue problem via the boundary element method, *Int. J. Numer. Methods Eng.* **36** (1993) 321–330.
12. H. Peters, N. Kessissoglou and S. Marburg, Modal decomposition of exterior acoustic-structure interaction, *J. Acoust. Soc. Am.* **133** (2013) 2668–2677.
13. S. K. Baydoun and S. Marburg, Investigation of radiation damping in sandwich structures using finite and boundary element methods and a nonlinear eigensolver, *J. Acoust. Soc. Am.* **147** (2020) 2020–2034.
14. M. El-Guide, A. Międlar and Y. Saad, A rational approximation method for solving acoustic nonlinear eigenvalue problems, *Eng. Anal. Bound. Elements* **111** (2020) 44–54.
15. T. Liang, J. Wang, J. Xiao and L. Wen, Coupled BE-FE-based vibroacoustic modal analysis and frequency sweep using a generalized resolvent sampling method, *Comput. Methods Appl. Mech. Eng.* **345** (2019) 518–538.
16. J.-P. Coyette, C. Lecomte, J.-L. Migeot, J. Blanche, M. Rochette and G. Mirkovic, Calculation of vibro-acoustic frequency response functions using a single frequency boundary element solution and a Padé expansion, *Acta Acust. United with Acust.* **85** (1999) 371–377.
17. J. Baumgart, S. Marburg and S. Schneider, Efficient sound power computation of open structures with infinite/finite elements and by means of the Padé-via-Lanczos algorithm, *J. Comput. Acoust.* **15** (2007) 557–577.

18. J. P. Tuck-Lee, P. M. Pinsky and H. L. Liew, Multifrequency analysis using matrix Padé-via-Lanczos, in *Computational Acoustics of NoisePropagation in Fluids-Finite and Boundary Element Methods*, eds. S. Marburg and B. Nolte (Springer, Berlin, Heidelberg, 2008), pp. 89–114.
19. S. Marburg and S. Schneider, Performance of iterative solvers for acoustic problems Part I: Solvers and effect of diagonal preconditioning, *Eng. Anal. Bound. Elem.* **27** (2003) 727–750.
20. M. L. Parks, E. de Sturler, G. Mackey, D. D. Johnson and S. Maiti, Recycling Krylov subspaces for sequences of linear systems, *SIAM J. Sci. Comput.* **28** (2006) 1651–1674.
21. S. Keuchel, J. Bierman and O. von Estorff, A combination of the fast multipole boundary element method and Krylov subspace recycling solvers, *Eng. Anal. Bound. Elem.* **65** (2016) 136–146.
22. Y. Liu, *Fast Multipole Boundary Element Method: Theory and Applications in Engineering* (Cambridge University Press, UK, 2009).
23. W. Hackbusch and B. Khoromskij, A sparse H-matrix arithmetic Part 2: Application to multi-dimensional problems, *Computing* **64** (2000) 21–47.
24. O. von Estorff, S. Rjasanow, M. Stolper and O. Zaleski, Two efficient methods for a multifrequency solution of the Helmholtz equation, *Comput. Vis. Sci.* **8** (2005) 159–167.
25. A. S. Wixom and J. G. McDaniel, Fast frequency sweeps with many forcing vectors through adaptive interpolatory model order reduction, *Int. J. Numer. Methods Eng.* **100** (2014) 442–457.
26. D. Panagiotopoulos, E. Deckers and W. Desmet, Krylov subspaces recycling based model order reduction for acoustic BEM systems and an error estimator, *Comput. Methods Appl. Mech. Eng.* **359** (2020) 112755.
27. S. K. Baydoun, M. Voigt, C. Jelich and S. Marburg, A greedy reduced basis scheme for multifrequency solution of structural acoustic systems, *Int. J. Numer. Methods Eng.* **121** (2020) 187–200.
28. L. Grasedyck, D. Kressner and C. Tobler, A literature survey of low-rank tensor approximation techniques, *GAMM-Mitt.* **36** (2013) 53–78.
29. S. K. Baydoun, L. Li, M. Voigt and S. Marburg, A low-rank iteration scheme for multi-frequency acoustic problems, in *Proc. 2018 ASME Int. Conf. Exposition on Noise Control Engineering*, eds. D. Herrin, J. Cuschieri and G. Ebbitt (INTERNOISE, Chicago, IL, USA, 2018), p. 1497.
30. D. Kressner and C. Tobler, Low-rank tensor Krylov subspace methods for parametrized linear systems, *SIAM J. Matrix Anal. Appl.* **32** (2011) 1288–1316.
31. J. Ballani and L. Grasedyck, A projection method to solve linear systems in tensor format, *Numer. Linear Algebr. Appl.* **20** (2012) 27–43.
32. S. Marburg, Developments in structural-acoustic optimization for passive noise control, *Arch. Comput. Methods Eng.* **9** (2002) 291–370.
33. K. Sepahvand, M. Scheffler and S. Marburg, Uncertainty quantification in natural frequencies and radiated acoustic power of composite plates: Analytical and experimental investigation, *Appl. Accoust.* **87** (2015) 23–29.
34. C. Runge, Über empirische Funktionen und die Interpolation zwischen äquidistanten Ordinaten, *Z. Math. Phys.* **46** (1901) 224–243.
35. H. A. van der Vorst, Bi-CGSTAB: A fast and smoothly converging variant of Bi-CG for the solution of nonsymmetric linear systems, *SIAM J. Sci. Stat. Comput.* **13** (1992) 613–644.
36. Y. Saad and M. H. Schultz, GMRES: A generalized minimal residual algorithm for solving nonsymmetric linear systems, *SIAM J. Sci. Stat. Comput.* **7** (1986) 856–869.
37. K. Lee, H. C. Elman and B. Sousedík, A low-rank solver for the Navier–Stokes equations with uncertain viscosity, *SIAM/ASA J. Uncertain. Quant.* **7** (2019) 1275–300.
38. S. Amini and N. D. Maines, Preconditioned Krylov subspace methods for boundary element solution of the Helmholtz equation, *Int. J. Numer. Methods Eng.* **41** (1998) 875–898.

39. H. Xiao and Z. Chen, Numerical experiments of preconditioned Krylov subspace methods solving the dense non-symmetric systems arising from BEM, *Eng. Anal. Bound. Elem.* **31** (2007) 1013–1023.
40. M. Hornikx, M. Kaltenbacher and S. Marburg, A platform for benchmark cases in computational acoustics, *Acta Acust. United with Acust.* **101** (2015) 811–820.
41. S. Marburg, A pollution effect in the boundary element method for acoustic problems, *J. Theor. Comput. Acoust.* **26** (2018) 1850018.
42. S. K. Baydoun and S. Marburg, Quantification of numerical damping in the acoustic boundary element method for two-dimensional duct problems, *J. Theor. Comput. Acoust.* **26** (2018) 1850022.
43. J. Baglama and L. Reichel, Augmented implicitly restarted Lanczos bidiagonalization methods, *SIAM J. Sci. Comput.* **27** (2005) 19–42.
44. N. Halko, P. G. Martinsson and J. A. Tropp, Finding structure with randomness: Probabilistic algorithms for constructing approximate matrix decompositions, *SIAM Rev.* **53** (2011) 217–288.
45. F. Negri, A. Manzoni and D. Amsallem, Efficient model reduction of parametrized systems by matrix discrete empirical interpolation, *J. Comput. Phys.* **303** (2015) 431–545.
46. A. Grim-McNally, E. de Sturler and S. Gugercin, Preconditioning parametrized linear systems, arXiv:1601.05883v4.
47. N. Dal Santo, S. Deparis, A. Manzoni and A. Quarteroni, Multi space reduced basis preconditioners for large-scale parametrized PDEs, *SIAM J. Sci. Comput.* **40** (2018) A954–A983.